

Experimental evidence on the development of scale invariance in the internal structure of self-affine aggregates.

C. M. Horowitz, M. A. Pasquale, E. V. Albano and A. J. Arvia

Instituto de Investigaciones Fisicoquímicas Teóricas y Aplicadas,

(INIFTA), CONICET, UNLP. Sucursal 4,

Casilla de Correo 16, (1900) La Plata. ARGENTINA. FAX

: 0054-221-4254642. E-mail : horowitz@inifta.unlp.edu.ar

Abstract

It is shown that an alternative approach for the characterization of growing branched patterns consists of the statistical analysis of frozen structures, which cannot be modified by further growth, that arise due to competitive processes among neighbor growing structures. Scaling relationships applied to these structures provide a method to evaluate relevant exponents and to characterize growing systems into universality classes. The analysis is applied to quasi-two-dimensional electrochemically formed silver branched patterns showing that the size distribution of frozen structures exhibits scale invariance. The measured exponents, within the error bars, remind us those predicted by the Kardar-Parisi-Zhang equation.

Interfaces grown under nonequilibrium conditions often show scaling behaviors and have attracted considerable interest[1, 2]. An intense theoretical activity based on the study of continuum as well as discrete growth models has provided scaling relationships between growth front roughness (i.e., the mean square fluctuation of interface position) and thickness, and upon changing the spatial scale of observation. Structures that preserve a similar morphology under an anisotropic magnification are termed self-affine. They play a key role in the rationalization of growth modes and the development of theories for growing aggregates. For a self-affine surface growing in a confined geometry of typical side L , the interface roughness (W) follows simple power-laws: $W \propto L^\alpha$ for $t \gg t_c$ and $W(t) \propto t^\beta$ for $t \ll t_c$, where $t_c \propto L^z$ is the crossover time between these two regimes. The scaling exponents α , β and z are called roughness, growth and dynamic exponents, respectively, and they are not independent, actually $z = \alpha/\beta$ [3]. These exponents allow us to identify the universality class of the system. In this context, experimental results from a large number of very different systems have been reported [1].

In contrast to the huge theoretical and experimental effort devoted to the understanding of the self-affine nature of interfaces, little attention has been drawn to the study of the internal (bulk) structure of growing systems. This approach is based on the fact that any growing system can effectively be rationalized on the basis of a treeing process; i.e., any growing structure can be thought as the superposition of individual trees[4, 5, 6, 7, 8, 9]. Those trees that spread out incorporating additional growing centers e.g., capturing particles, developing new branches, are said to be alive. In contrast, other trees that may stop growing due to shadowing by surrounding growing trees are termed dead trees. The structure of dead trees remains frozen because it cannot be modified by any further growth. Considering that relationships among exponents relevant for the distribution of dead trees and the standard scaling exponents have been established theoretically and tested numerically [4, 5, 6, 7, 8, 9, 10], this approach may provide an alternative (experimental) method for characterizing growing systems. Thus, this method could be used in any experimental situation where the competitive dynamics of growing trees leading to frozen structures can be observed. A promising application of this method could be the electrochemical deposition of metals in thin cells. This rather simple experimental technique offers the possibility to observe a variety of self-affine patterns, ranging from dense branching to diffusion-limited aggregation [11, 12, 13, 14]. Another application could be to study polycrystalline thin film growth by

scanning tunneling microscopy [15, 16] and atomic force microscopy [17]. In these cases the direct evaluation of the number of crystallites as a function of the deposit height would account for the number of frozen crystallites (i.e., the trees of the growing aggregate) and the crystallite size distribution can then be evaluated. Also, self-organized patterns formed upon bacterial colony growth, which can be rationalized in terms of competing knotted-branched structures [18], may provide an interesting application of the proposed method.

Despite the fact that internal structure analysis has been developed theoretically and tested numerically in various growing models, its application to real systems is very poor in the literature. The goal of this paper is to fill this gap by characterizing quasi-two-dimensional electrodeposited silver patterns produced under mass transfer kinetic control. Silver electrodeposition was carried out at two different cathode-anode potentials, under the same kinetic control mechanism. Although long range interactions are present in a number of metal electrodeposition processes, in previous work it was shown that the standard exponent α , β and z derived from growth patterns obtained under conditions similar to those reported here, asymptotically approach the values predicted by the Kardar-Parisi-Zhang (KPZ) universality class [19, 20]. In this work we show that the internal structure statistical analysis of silver electrodeposits renders scaling relationships and relevant exponents that, within the error bars, also remind us those exponents predicted by the KPZ universality class.

Silver electrodeposition was performed using a quasi-2D rectangular cell with a vertical parallel plate electrode arrangement. The cell consisted of two optical glass plates placed horizontally and separated by 0.025 cm. The cathode and anode were made of a silver foil, 99.9 % purity, 0.025 cm thick. The cathode width was 9 cm and the cathode to anode distance was 4 cm. Further details of the experimental setup can be found in Ref.[20]. Aqueous solution 0.01 M silver sulfate / 0.5 M sodium sulfate / 0.01 M sulfuric acid, saturated with nitrogen, freshly prepared utilizing analytical grade reagents and Milli-Q water, was employed. The electrodeposition was run under two different constant cathode-anode potentials, i.e., $\Delta E_{c-a} = -0.80$ V, and $\Delta E_{c-a} = -1.20$ V, employing a Radiometer Volta-master 32 potentiostat. Images of whole growth patterns were acquired at the end of each experiment using a charge coupled device video camera, Hitachi 220, coupled to a computer equipped with a frame grabber and image analyzer, Contron Electronics KS. After binarization, the spatial resolution of the images was $31.25\mu m$ per pixel. A program written in

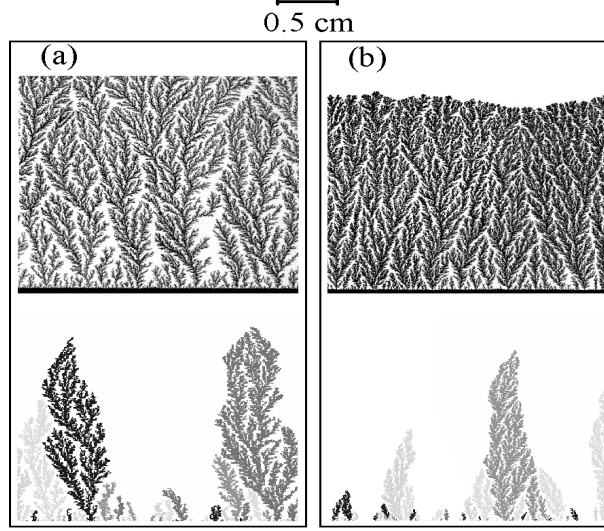


FIG. 1: Silver pattern electrodeposits from 0.01M silver sulfate / 0.5 M sodium sulfate / 0.01 M sulfuric acid. (a) at $\Delta E_{c-a} = -0.80$ V, electrodeposition time 110 min and (b) at $\Delta E_{c-a} = -1.20$ V, electrodeposition time 90 min . The dead trees corresponding to both patterns are shown at the bottom of each figure

Fortran was used to distinguish internal trees separately and to evaluate the distribution of dead trees.

Silver electrodeposition is one of the fastest electrochemical reactions due to its high exchange current density value [21]. Despite the use of a supported electrolyte in the solution, the electrical resistances of quasi-two-dimensional cells are rather high. Thus the applied potential between electrodes affects the electrochemical process producing a bias for the impinging particles that arrive at the interface. It should be stressed that for the working conditions employed in this work, the electrochemical reaction is under mass transfer control, i.e., the convective-diffusion flux plays an important role in determining the morphology of the obtained patterns[22, 23].

Figure 1 shows silver patterns, with their final structures of dead trees, obtained at two constant cathode-anode potentials. These patterns consist of an early thin, rough deposit, followed by a columnar formation with a preferred growth along the direction of the electric field. After a certain deposition time, which decreases as ΔE_{c-a} is shifted negatively, separated tree-like formations resulting in a dense branching with the same preferred growth direction, partially screening the growth of neighbor columns, can be observed. The mor-

phological characteristics of both aggregates are significantly different. Thus, the density of trees and the aggregate apparent density seem to increase as ΔE_{c-a} is changed from -0.80V to -1.20V .

The analysis of the internal structure of the growth patterns is performed following the procedure outlined in reference [10]. Pointing our attention to dead trees of size s (s is the number of particles belonging to the tree), one has that both, the rms height (h_s) and the rms width (w_s) of trees obey simple power-laws given by

$$h_s \propto s^{\nu_{\parallel}}, \quad (1)$$

and

$$w_s \propto s^{\nu_{\perp}}, \quad (2)$$

where ν_{\parallel} and ν_{\perp} are the correlation length exponents parallel and perpendicular to the main growing direction of the aggregate [8], respectively.

Furthermore, during the competition between trees along the evolution of the aggregate, the existence of large neighboring trees inhibit the growing of smaller ones. This competing process ultimately leads to the death of some trees that become frozen within the underlying aggregate. These prevailing large trees continue the competition within more distant trees in a dynamic process. Since this situation takes place on all scales, it is reasonable to expect that the tree size distribution (n_s) should also exhibit a power-law behavior, so that

$$n_s \sim s^{-\tau}, \quad (3)$$

where τ is an exponent.

The evaluation of h_s , w_s and n_s was performed using ten different samples for each set of experimental conditions. Thus, these quantities were evaluated using 1056 trees for $\Delta E_{c-a} = -0.80\text{ V}$ and 1260 trees for $\Delta E_{c-a} = -1.20\text{ V}$. In these measurements, the tree size s was taken as the number of pixels belonging to the tree. The dependences of h_s and w_s on s are shown in the log-log plots of figures 2 and 3, respectively. In these figures, each point has been obtained averaging over the number of trees with size s inside a range $s^* - ds, s^* + ds$. Thus, the quoted error bars only account for the method applied to that procedure, and the total error is expected to be greater.

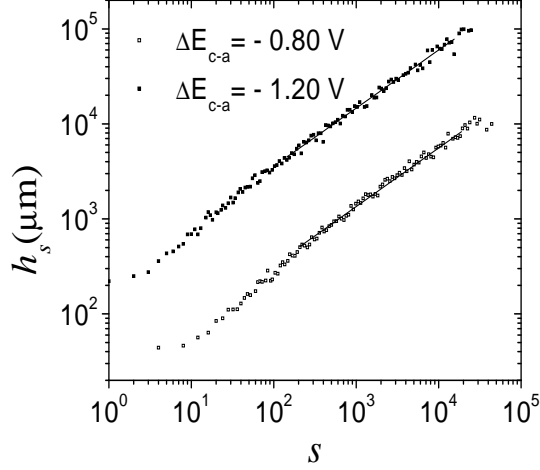


FIG. 2: Log-log plots of rms height of the trees as a function of the tree size s . The rms height is measured in μm and the size s is given by the number of pixels of each tree. The result at $\Delta E_{c-a} = -1.20$ V has been shifted by a factor 10 for clarity.

It is worth mentioning that, as follows from these figures, in most cases power-laws extends over more than two decades. Also, plots for both values of ΔE_{c-a} are almost parallel, indicating the same underlying scaling behavior. For $\Delta E_{c-a} = -0.80$ V, the best fit of the data gives $\nu_{\parallel} = 0.63 \pm 0.03$ and $\nu_{\perp} = 0.46 \pm 0.06$, while for $\Delta E_{c-a} = -1.20$ V one has $\nu_{\parallel} = 0.62 \pm 0.03$ and $\nu_{\perp} = 0.46 \pm 0.06$. Notice, that the error in the estimation of the exponents is the standard one, that follows from the fitting data.

On the other hand, the tree size distributions measured for both values of ΔE_{c-a} (see figure 4) are fully consistent with equation (3). Log-log plots of n_s versus s indicate again the same scaling behavior, irrespective of ΔE_{c-a} . The best fit of the data gives $\tau = 1.37 \pm 0.04$. As in the case of ν_{\parallel} and ν_{\perp} the error only reflect the statistical error.

For self-affine aggregates with geometrical dimension D growing on a d -dimensional substrate, it has been already established that [8]

$$\tau = 2 - \nu_{\parallel}(D - d). \quad (4)$$

For the experimental conditions used in this work one has $D = 2$ and $d = 1$, therefore equation (4) becomes

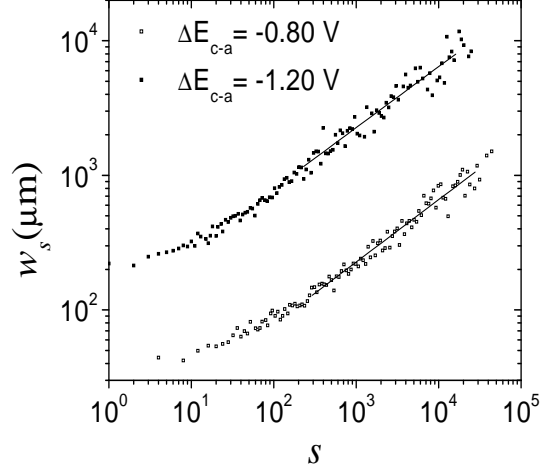


FIG. 3: Log-log plots of rms width of the trees as a function of the tree size s . The rms width is measured in μm and the size s is given by the number of pixels of each tree. The result at $\Delta E_{c-a} = -1.20$ V has been shifted by a factor 10 for clarity.

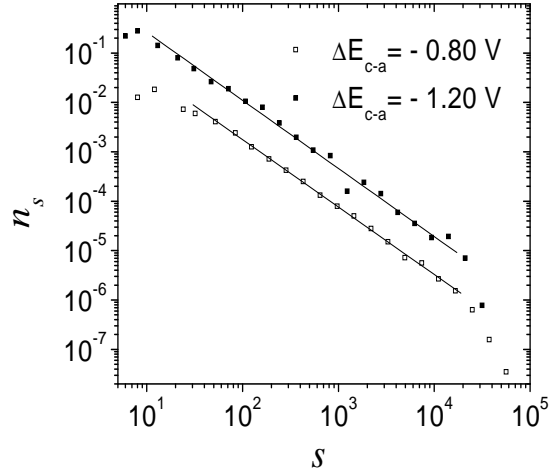


FIG. 4: Log-log plots of the tree size distribution, where the size s is given by the number of pixels of each tree. The result at $\Delta E_{c-a} = -1.20$ V has been shifted by a factor 10 for clarity.

$$\tau + \nu_{\parallel} - 2 = 0. \quad (5)$$

In principle, one lacks any physical argument to expect that a compact (constant apparent density) aggregate may result from the addition of compact trees. In fact, the volume of

trees of size s (v_s) scales, for any dimension, as

$$v_s \sim h_s w_s^d \sim s^{\nu_{\parallel} + d\nu_{\perp}}, \quad (6)$$

and therefore, it is useful to define a relationship $v_s \sim s^{\pi}$ between the volume and the number of particles, where π is an exponent, so that

$$\nu_{\parallel} + d\nu_{\perp} = \pi, \quad (7)$$

where for compact trees one has $\pi = 1$ while for non-compact (fractal) trees $\pi > 1$.

Finally, identifying the correlation length perpendicular to the main growing direction with w_s and the time with h_s , one has that the dynamic exponent $z = \alpha/\beta$ is given by [9]

$$z = \nu_{\parallel}/\nu_{\perp}. \quad (8)$$

Depending on the operating conditions, metal electrodeposition processes involve a number of competitive effects that are considered in both non-local and local models used to describe growth pattern kinetics. Thus, when the working conditions involve both electromigration and activated electron transfer limited kinetics, as it appears to be the case of zinc electrodeposition, the value $\tau \simeq 1.54$ has been obtained [6]. This figure has been interpreted by the diffusion-limited aggregation (DLA) model [24]. For our working conditions, where silver electrodeposition takes place under almost exclusively convective-diffusion rate control (negligible electromigration and electron transfer overvoltage), the exponents resulting from the experimental data are assembled in Table 1. It should be stressed that the formulation of a detailed model describing the complex processes involved upon silver electrodeposition is far beyond the aim of this report. However, well established concepts in the field of statistical physics, that are very useful in the study of phase transition, self-similar and self-affine structures as in the present case, allow us to rationalize even very complex systems into few universality class. Of course, systems within the same universality share the same exponents. For this reason, it is useful to check experimentally evaluated exponents to those of the simplest models representing each universality. Thus, for the sake of comparison, the values of the exponents predicted by the Edward Wilkinson (EW) and the Kardar-Parisi-Zhang (KPZ) models are included in Table I. The values of these exponents do not depend

on ΔE_{c-a} . Considering error bars, values of ν_{\perp} and z are very close to those expected from the KPZ universality class. It is worth noting that from our experiments the value $\tau = 1.37$ (4) approaches that of the KPZ model instead of $\tau \simeq 1.55$, predicted by the DLA model. Besides, the value of $\pi \simeq 1$ indicates that trees behave as constant apparent density, compact objects (non fractal). To check the consistency of the method employed, the relationship given by equation (5) was evaluated using the experimental exponents obtaining a good agreement with the theory.

Summing up, the application of the internal structure analysis based method to experimental data allows us to conclude that the evaluation of treeing statistics is a suitable method for the characterization of growing aggregates. Furthermore, the exponents derived from electrodeposited silver patterns are consistent with those corresponding to the KPZ universality class. It is expected that the statistical analysis of bulk structures may become a useful tool for the characterization of growing aggregates, particularly in those cases where the topology of the interface is not accessible experimentally.

Acknowledgments: This work was supported by CONICET, UNLP and ANPCyT (Argentina).

-
- [1] A. L. Barabasi and H. E. Stanley, in "Fractal Concepts in Surface Growth." Cambridge University Press, Cambridge (1995).
 - [2] J. Kertész and T. Vicsek, Self-Affine Interfaces, in Fractals in Science, Edited by A. Bunde and S. Havlin. Springer-Verlag, Berlin (1995), Page 89.
 - [3] F. Family, T. Vicsek, J. Phys. A., **18**, L75 (1985).
 - [4] Z. Rácz and T. Vicsek, Phys. Rev. Lett. **51**, 2382 (1983).
 - [5] P. Meakin, Phys. Rev. B **30**, 4207 (1984).
 - [6] M. Matsushita, Y. Hayakawa, and Y. Sawada Phys. Rev. A **32**, 3814 (1985).
 - [7] P. Meakin, J. Phys. A: Math. Gen **20**, L1113 (1987).
 - [8] M. Matsushita and P. Meakin, Phys. Rev. A **37**, 3645 (1988).
 - [9] J. Krug and P. Meakin, Phys. Rev. A **40**, 2064 (1989).
 - [10] F. Romá, C. M. Horowitz and E. V. Albano. Phys. Rev. E. **66**, 066115 (2002).
 - [11] M. Matsushita, in The Fractal Approach to the Heterogeneous Chemistry, edited by D. Avnir (Wiley, New York, 1989), p. 161 and references therein.
 - [12] Y. Sawada, A. Dougherty, and J. P. Gollub Phys. Rev. Lett. **56**, 1260 (1986).
 - [13] D. Barkey, F. Oberholtzer, and Q. Wu, Phys. Rev. Lett. **75**, 2980 (1995).
 - [14] J. Elezgaray, C. Léger and F. Argoul, Phys. Rev. Lett. **84**, 3129 (2000).
 - [15] E. V. Albano, R. C. Salvarezza, L. Vázquez, and A. J. Arvia. Phys. Rev. B. **59**, 7354 (1999).
 - [16] L. Vázquez, R. C. Salvarezza, E. V. Albano, A. J. Arvia, A. Hernández Creus, R. Levy and J. Albella. Adv. Mat. **4**, 89 (1998).
 - [17] F. Ojeda, R. Cuerno, R. C. Salvarezza and L. Vázquez, Phys. Rev. Lett. **84**, 3125 (2000).
 - [18] E. Ben-Jacob *et al*, Nature (London) **368**, 46 (1994).
 - [19] P. Schilardi, O. Azzaroni, R. C. Salvarezza and A. J. Arvia, Phys. Rev. B, **59**, 4638 (1999).
 - [20] M. A. Pasquale, S. L. Marchiano and A. J. Arvia, J. Electroanal. Chem. **532**, 255 (2002).
 - [21] H. Gerischer and R. P. Tischer, Z. Electrochem. **61**, 1159 (1957).
 - [22] P. Garik, D. Barkey, E. Ben-Jacob, E. Bochner, N. Broxholm, B. Miller, B. Orr, R. Zamir, Phys. Rev. Lett. **62**, 2703 (1989).
 - [23] D. Barkey, P. Garik, E. Ben-Jacob, B. Miller, B. Orr, J. Electrochem. Soc. **139**, 1044 (1992).
 - [24] T. A. Witten and L. M. Sander, Phys. Rev. Lett. **47**, 1400 (1981).

TABLE I: Scaling exponents ν_{\perp} , ν_{\parallel} , τ determined from electrodeposited silver patterns and the predictions corresponding to both the KPZ and EW universality classes are shown in the 2nd, 3rd and 4th columns, respectively. A test of equation (5) is shown in the 5th column. Values of π (equation (7)) and z (equation (8)) are shown in the 6th and 7th columns, respectively.

System	ν_{\perp}	ν_{\parallel}	τ	$\tau + \nu_{\parallel} - 2$	π	z
Experimental ($\Delta E_{c-a} = -0.80$ V)	0.46(6)	0.63(3)	1.37(4)	0.00(5)	1.09(7)	1.4(2)
Experimental ($\Delta E_{c-a} = -1.20$ V)	0.46(6)	0.62(3)	1.37(4)	0.01(5)	1.08(7)	1.4(2)
KPZ universality class	0.40	0.60	1.40	0	1	3/2
EW universality class	0.35	0.65	1.35	0	1	2